MIT
CEEPR   Center for Energy and Environmental Policy Research

Reductions in ozone concentrations due to controls on
variability in industrial flare emissions in Houston, Texas

by
Junsang Nam, Mort Webster, Yosuke Kimura,
Harvey Jeffries, William Vizuete, David T. Allen

07-009   August 2007

**A Joint Center of the Department of Economics, Laboratory for Energy
and the Environment, and Sloan School of Management**

Reductions in ozone concentrations due to controls on variability in industrial flare emissions in Houston, Texas

Junsang Nam[1], Mort Webster[2*], Yosuke Kimura[1], Harvey Jeffries[3], William Vizuete[3], David T. Allen[1]

[1] University of Texas, Center for Energy and Environmental Resources, 10100 Burnet Road, M/S R7100, Austin, TX 78758

[2] Massachusetts Institute of Technology, Department of Earth, Atmosphere, and Planetary Sciences, E40-408, 77 Massachusetts Avenue, Cambridge, MA 02139

[3] University of North Carolina, Department of Environmental Sciences and Engineering, School of Public Health, Chapel Hill, NC 27599

*Corresponding author, fax 617-253-9845; email: mort@mit.edu

Abstract

High concentrations of ozone in the Houston/Galveston area are associated with industrial plumes of highly reactive hydrocarbons, mixed with NO_x. The emissions leading to these plumes can have significant temporal variability, and photochemical modeling indicates that the emissions variability can lead to increases and decreases of 10-50 ppb, or more, in ozone concentrations. Therefore, in regions with extensive industrial emissions, accounting for emission variability can be important in accurately predicting peak ozone concentrations, and in assessing the effectiveness of emission control strategies. This work compares the changes in ozone concentrations associated with two strategies for reducing flare emissions in Houston, Texas. One strategy eliminates the highest emission flow rates, that occur relatively infrequently, and a second strategy reduces emissions that occur at a nearly constant level. If emission variability is accounted for in air quality modeling, these control scenarios are predicted to be much more effective in reducing the expected value of daily maximum ozone concentrations than if similar reductions in the mass of emissions are made and constant emissions are assumed. The change in the expected value of daily maximum ozone concentration per ton of emissions reduced, when emissions variability is accounted for, is 5-10 times the change predicted when constant (deterministic) inventories are used.

Keywords: Photochemical Grid Model, highly reactive volatile organic compounds (HRVOC), ozone, uncertainty analysis.

Introduction

The Houston/Galveston (HG), area, like many large urban areas in the United States, exceeds the National Ambient Air Quality Standards (NAAQS) for ground-level ozone with concentrations averaged over 1 hour and 8 hours. Unlike other urban areas in the United States, however, changes in observed ozone concentrations in the HG area are rapid (up to 200 ppb/hr) and efficient (up to 10-20 moles ozone formed per mole of NOx consumed). These unique characteristics of ozone formation in the HG area are associated with plumes of reactive hydrocarbons, emanating from the industrial Houston Ship Channel area (Kleinman et al., 2003; Ryerson et al., 2003). Therefore, understanding industrial emissions, particularly of reactive hydrocarbons, is critical in the development of control measures for mitigation of high ozone concentrations in the area.

Industrial emissions of hydrocarbons, from sources other than electricity generating units (non-EGU), have traditionally been assumed to be continuous at constant levels for air quality regulation and photochemical modeling purposes. However, ambient observations and industrial process data from the HG area have shown that non-EGU industrial emissions of hydrocarbons have significant temporal variability (Murphy and Allen, 2005; Webster, et al., 2007). Variability in non-EGU industrial emissions of hydrocarbons in the HG area can be ascribed to both the occurrence of episodic emission events and variable continuous emissions. The episodic emission events are non-routine discrete emission events, of more than permitted amounts, with reporting required under Texas law. Episodic events occur relatively infrequently; an emission event of more than 1000 kg occurs, on average, a few times a week somewhere among the hundreds of facilities and the thousands of non-EGU industrial emission points in the Houston area (Murphy and Allen, 2005). So, at any single facility or process unit, an emission event is a rare occurrence, but collectively, over the entire region, large emission events (>1000 kg) occur weekly. Nam et al. (2006) performed photochemical modeling of hundreds of emission events, and concluded that only a small percentage of the events lead to large increases in ozone concentrations. Approximately 1.5% of emission events produced more than 10 ppb of additional ozone, and 0.5% of emission events produced more than 70 ppb of additional ozone, compared to base case photochemical modeling simulations with no emission events.

Variable continuous emissions are not as significant in magnitude as emission events, but occur at all times, at all facilities and process units, and therefore also have the potential to

increase the magnitude of ozone concentration in the HG area.   Webster et al. (2007) described the variability in routine hydrocarbon emissions from non-EGU industrial sources in terms of three emission modes: nearly constant emissions, routinely variable emissions and allowable (within permitted levels) episodic emissions. Each mode was described for multiple sources, such as flares, cooling towers, and process vents and area–wide emissions from these industrial sources were modeled for the HG area. Air quality simulations indicated that variability in industrial emissions had the potential to cause increases and decreases of 10-50 ppb, or more, in ozone concentration, as compared to simulations with the same total emissions, but industrial non-EGU emissions that are assumed to be constant. The largest of these differences were predicted to be confined to small areas (10-20 km^2), but the emission variability also had the potential to increase region wide maxima in ozone concentrations by up to 12 ppb.

These results indicate that variability in industrial non-EGU emissions may be just as important to control as discrete emission events and the average magnitude of the emissions. This work will examine the impacts of controls on the modes of emissions considered by Webster, et al (2007): nearly constant, routinely variable, and allowable episodic. Emissions from flares will be used as a case study. Flares were chosen for focus because they constitute a significant fraction of industrial emissions in the HG area, and their variability was well characterized by Webster, et al (2007). In addition, Flare Minimization Plans (FMPs) have been prepared by petroleum refineries in the San Francisco Bay Region, as required by the Bay Area Air Quality Management District (BAAQMD, 2005, 2006). These minimization plans provide insight into the types of controls that can be used to reduce different modes of flare emission variability.

Methods

The stochastic emission inventory for the HG area

Webster et al. (2007) indicated that continuous industrial emissions of VOC have significant temporal variability and the variability is composed of multiple components, including nearly constant, routinely variable, and allowable episodic emissions.   As shown in Figure 1, emission events above permitted levels also occur, but the analysis presented in this work will consider only emissions that are within permitted values. Nam et al (2006) report on the impacts of discrete emission events above permitted levels.

Webster, et al (2007) simulated industrial emissions using probability distribution functions (PDF) for three emission modes (nearly constant, routinely variable and allowable episodic). The choice of this approach was based on data from flares and cooling towers in the HG area. An example of the mass flow rates and the variability in those flow rates associated with nearly constant, routinely variable and allowable episodic emissions are shown in Figure 2. The data are for one of 10 industrial flares on which Webster, et al. (2007) collected data. Figure 2a shows the original probability distributions for flare flow rates, as developed by Webster, et al. (2007). Figure 2b shows the modified distributions used in this work, which are described in more detail below.

Table 1 reports the characteristic parameters of the probability distributions for the emission modes for 10 flares and 2 cooling towers on which data were collected. To develop an emission inventory for all industrial sources in the HG area, based on these data, Webster, et al (2007) assigned all of the flares and cooling towers in the HG area one of the unit operation models. For example, all flares were randomly assigned the variability in emissions of one of the ten flare models. The mean of the emission variability model was scaled so that it matched the mean emissions of the specific flare under consideration. Similarly, all cooling towers were assigned one of the cooling tower models and all process vents were assigned the process vent model. For cooling towers and process vents, all emissions except VOCs were kept at their original, constant levels. For flares, both VOC and NO_x emissions were assumed to scale with flow rate having the same pattern of variability. Details on the development of the stochastic emission inventory generator and application of the stochastic inventory to the HG area have been described by Webster et al. (2007).
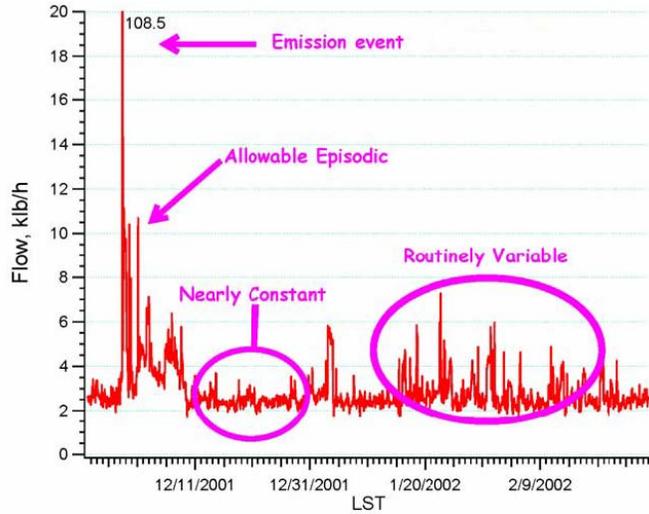
Figure 1. Components of mass flow rates to a flare at an industrial facility in the HG area: nearly constant, routinely variable, allowable episodic, and emission event in order of magnitude (Webster et al., 2007).
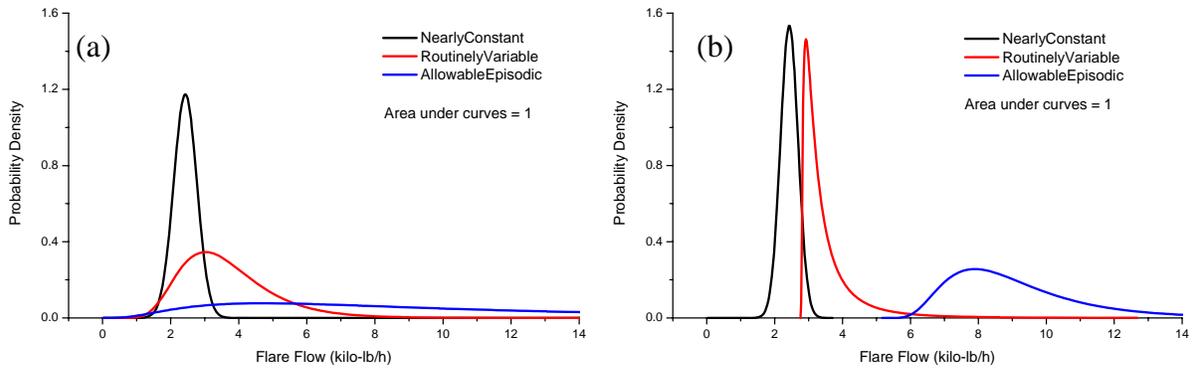

Figure 2. PDFs for each component of emissions from the flare in Figure 1 in (a) the original version of the stochastic inventory generator (Webster et al., 2007); $f(x;\mu;\sigma) = \dfrac{e^{-(ln\ x-\mu)^2/(2\sigma^2)}}{x\sigma\sqrt{2\pi}}$ for routinely variable and allowable episodic components and (b) the updated version of the stochastic inventory generator (Webster, 2007); $f(x;\mu;\sigma) = \dfrac{e^{-(ln(x-shift)-\mu)^2/(2\sigma^2)}}{(x-shift)\sigma\sqrt{2\pi}}$ for routinely variable and allowable episodic components.

Table 1. Fitted parameters for observations from emission sources

Source Name (Type)	Component	Normal or Lognormal	Mean or Mean (LN Value)*	Standard deviation	Normalized proportion	Transition Matrix			Shift	Expected values
Flare1	1	N	2.43	0.26	0.603	0.883	0.115	0.001	0	2.430
(FL)	2	LN	-0.798	1.05	0.389	0.179	0.813	0.008	2.76	3.541
	3	LN	1.26	0.5	0.008	0.085	0.38	0.535	5.14	9.135
Flare2	1	N	1.97	0.64	0.544	0.798	0.196	0.005	0	1.970
(FL)	2	LN	0.54	0.97	0.426	0.252	0.729	0.02	2.81	5.557
	3	LN	-0.75	1.65	0.029	0.048	0.333	0.619	11	12.843
Flare5	1	LN	6.8	0.305	0.7632	0.951	0.022	0.027	42.64	983.2
(FL)	2	N	2017	114.8	0.061	0.29	0.557	0.154	0	2017.3
	3	LN	5.98	0.72	0.1758	0.113	0.058	0.829	2153.19	2665.6
FCCU	1	N	21.1	3.01	0.9063	0.997	0.002	0.001	0	21.10
(FL)	2	N	33.67	2.14	0.0719	0.032	0.958	0.01	0	33.67
	3	LN	0.95	0.69	0.0217	0.003	0.058	0.939	37.56	40.84
General	1	N	21.4	1.51	0.9462	0.99	0.009	0.001	0	21.40
Service1	2	LN	-0.572	1.44	0.0402	0.218	0.762	0.02	23.99	25.58
(FL)	3	LN	0.404	1.41	0.0135	0.046	0.068	0.886	28.85	32.90
General	1	N	17.08	0.94	0.67	0.97	0.027	0.003	0	17.08
Service2	2	N	19.18	0.16	0.25	0.072	0.869	0.059	0	19.18
(FL)	3	LN	-1.61	1.48	0.08	0.022	0.186	0.792	19.48	20.08
HCF	1	N	2.41	0.62	0.974	0.989	0.011		0	2.410
(FL)	2	LN	-0.3	0.64	0.026	0.426	0.574		4.01	4.919
Low	1	N	24.64	0.918	0.6918	0.988	0.012	0	0	24.64
Pressure	2	LN	0.158	0.712	0.298	0.027	0.972	0.001	25.78	27.29
(FL)	3	LN	0.079	0.558	0.0102	0.011	0.039	0.95	34.76	36.02
Merox	1	N	31.9	16.23	0.056	0.896	0.091	0.012	0	31.90
(FL)	2	N	500.4	89.45	0.914	0.006	0.991	0.003	0	500.4
	3	LN	4.891	0.242	0.03	0.019	0.082	0.899	622.5	759.5
Olefins	1	N	1.67	0.41	0.661	0.973	0.027	0	0	1.670
Flare	2	LN	0.98	0.51	0.327	0.053	0.944	0.003	2.3387	5.373
(FL)	3	LN	0.38	1.02	0.012	0.045	0.045	0.909	16.88	19.34
Cooling	1	N	0.065	0.029	0.656	0.746	0.19	0.063	0	0.065
Tower1	2	LN	-2.778	1.023	0.194	0.623	0.295	0.082	0.13247	0.237
(CT)	3	LN	-1.811	0.945	0.15	0.298	0.085	0.617	0.39282	0.648
Cooling	1	N	0.228	0.077	0.29	0.835	0.155	0.01	0	0.228
Tower2	2	N	0.671	0.131	0.438	0.095	0.73	0.176	0	0.671
(CT)	3	LN	-1.013	0.963	0.272	0.022	0.272	0.707	0.86246	1.440
STs/FUs	1	LN	-0.15	0.56	1	NA				1.007

*Emissions in klb/hr, except for Flare 5 and Merox flare which are lb/hr

The goal of this work is to examine the effect of placing controls on the variability of emissions from flares. To model these control strategies, it was necessary to modify the stochastic emission inventory generator. The original version of the stochastic emission inventory generator (Webster et al., 2007) randomly selects emission mode (from nearly constant, routinely variable, and allowable episodic modes), duration in the mode and, then, emission rates. The selections of emission modes, durations in each mode, and emission rates were based on probability distribution functions (PDFs) of observations. The modification made in the revised version of the stochastic inventory generator is to use the transition matrix, shown in Table 1, to determine the probability of transition from the current mode to the next mode for every time step. This method assumes that emissions are being generated by a Markov process. A Markov process is a system in which the conditional probability distribution over future states is dependent on the current state of the process. In the transition matrix, the row index (i) represents the current mode and the column index (j) represents the next mode; the entries in the matrix represents the probability of transition from the current mode (i) to the next mode (j), P_{ij}. For example, for Flare 1 shown in Table 1, probabilities of transition from current mode 1 to modes 1, 2, and 3, in the next time step, are 0.883, 0.115, and 0.001, respectively. This simplified algorithm allows the model to be readily adapted to model control strategies that eliminate one or more modes. For example, modeling the elimination of allowable episodic emissions only requires that the probability of the system initially being in that mode be set to zero and that the probability of transition to that mode be set equal to zero.

In addition, the revised version of the stochastic inventory generator shifts the distributions for lognormal components of the models. Lognormal distributions are, in general, positively skewed; they have their peak likelihood at relatively small values and have long tails in the probability distribution at higher values. The control scenarios outlined later in this paper are effective in only relatively narrow emission ranges (corresponding to narrow ranges of flare flow rates). Therefore the lognormal distributions were recast so that they represented narrower flow rate bands. Figure 2 shows probability distribution functions (PDFs) for each component of emissions from the flare in Figure 1 in the original version and the revised version of the stochastic inventory generator. The revised flow rate bands have narrower distributions. To accomplish these changes, the PDFs were modified in the following ways:

7

$$f(x;\mu;\sigma) = \frac{e^{-(ln(x-shift)-\mu)^2/(2\sigma^2)}}{(x-shift)\sigma\sqrt{2\pi}}, \text{ instead of } f(x;\mu;\sigma) = \frac{e^{-(ln\ x-\mu)^2/(2\sigma^2)}}{x\sigma\sqrt{2\pi}}$$

This change allows the model to more effectively eliminate or reduce emissions in a specified flare flow rate regime. Figure 3 shows mass flow rates to the flare in Figure 1 simulated with the original version and the revised version of the stochastic inventory generator and observed mass flow rates to this flare. As described in the results section of this paper, the revised stochastic emissions generator leads to similar distributions in predicted ozone concentrations.
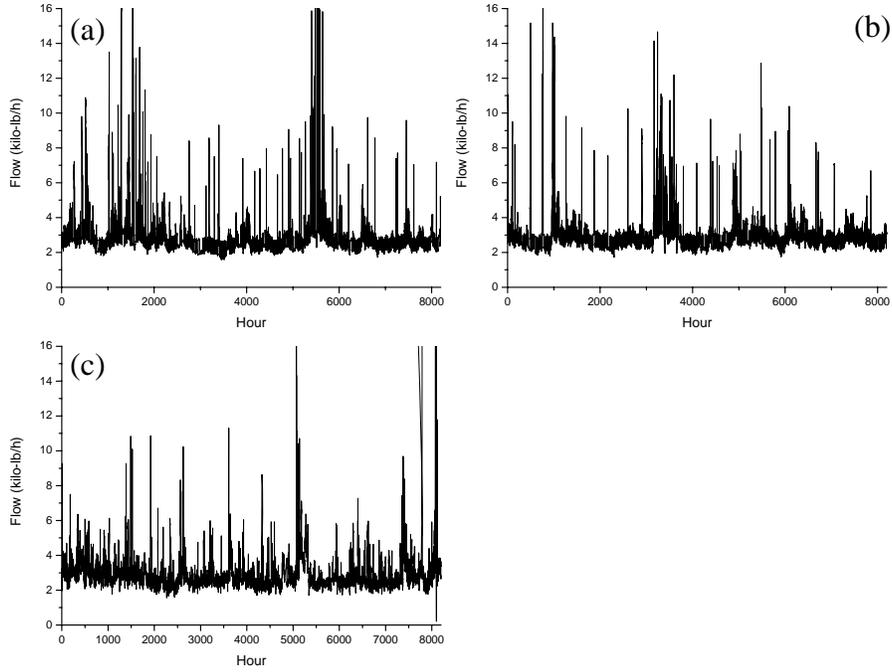
Figure 3. (a) Time series of flare flow in Figure 1 simulated with original version of the stochastic inventory generator. (b) Time series of flare flow in Figure 1 simulated with the revised version of the stochastic inventory generator. (c) Time series of actual flare flow.

Control strategies associated with variability in industrial hydrocarbon emissions

In order to understand how flare emissions can be reduced, and how those emission reductions can be modeled, it is useful to have a conceptual understanding of how a typical industrial flare system works. In many industrial operations, a flare serves multiple process units. The flare collects these multiple inputs through a collection system, or plenum, that is maintained at low pressure so that the plenum will always be at a lower pressure than the process units that it serves. Many systems that are designed to flare material with fuel value (e.g., fuel gases) are served by a compressor, so that some of the flare gases can be recycled to the facility's fuel system, which is maintained at a higher pressure than the flare system. If the flow to the flare is less than the capacity of the compressor, fuel gases that are sent to the flare system are recompressed and recycled to a process unit that uses fuel gas. If the flow is larger than can be handled by the compressor, then the fuel gas is flared. This fuel flare system is shown conceptually in Figure 4.
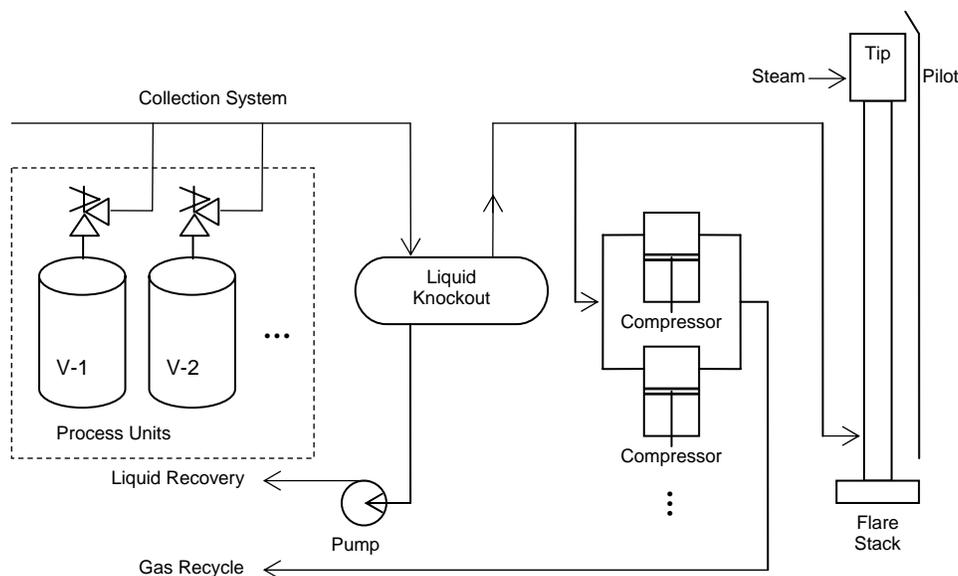

Figure 4. Conceptual diagram for a typical refinery flare system (Shell Oil Products US, 2006)

With this conceptual model of flare systems in mind, two options for reducing flare emissions are (1) to add temporary storage for flared gases, so that if the flow rate to the flare goes above the capacity of the compressor, the gases can be temporarily stored, and (2) to add additional compressor capacity to a flare system.

In general, adding storage capacity for flared gases is expensive. However, temporary storage is sometimes available during start-up, shut-down and maintenance activities. A flare minimization scenario that has been reported in Flare Minimization Plans by petroleum refineries is to use process vessels that are temporarily empty during start-up, shut-down and scheduled maintenance as temporary storage for gases that would otherwise be flared during these events. This requires careful scheduling of operations during start-ups, shut-downs and maintenance activities, but it can reduce what are often large flaring events.

Adding additional compressor capacity to a flare system is another option for increasing the amount of fuel gas that is recycled. Adding compressor capacity can also be expensive, if the compressor only recovers fuel during relatively rare emission events. However, if compressor capacity can be added to capture and recycle nearly constant flare emissions, it becomes more cost effective.

Based on these ideas, two approaches were evaluated for reducing flare emissions. The first approach is to control the large magnitude, infrequent emissions from flares (allowable episodic mode). This corresponds to eliminating large flaring events during start-up, shut-down and maintenance activities. In modeling this approach, the allowable episodic emissions for all of the flares in the HG area were assumed to be eliminated. For this task, the stochastic inventory generator was modified to reflect this control approach, as shown in Table 2, and the stochastic inventory generated from this modified model was used to investigate the impacts on ozone formation of this emission control approach.

Table 2. Parameters used to develop stochastic emissions with allowable episodic emissions from flares eliminated.

Source Name (Type)	Component	Normal or Lognormal	Mean or Mean (LN Value)	Standard deviation	Normalized proportion	Transition Matrix			Shift	Expected value
Flare1	1	N	2.43	0.26	0.608	0.884	0.115		0	2.43
(FL)	2	LN	-0.798	1.05	0.392	0.179	0.821		2.76	3.54
Flare2	1	N	1.97	0.64	0.561	0.803	0.196		0	1.97
(FL)	2	LN	0.54	0.97	0.439	0.252	0.749		2.81	5.56
Flare5	1	LN	6.8	0.305	0.926	0.978	0.022		42.64	983.2
(FL)	2	N	2017	114.8	0.074	0.29	0.711		0	2017
FCCU	1	N	21.1	3.01	0.926	0.998	0.002		0	21.1
(FL)	2	N	33.67	2.14	0.074	0.032	0.968		0	33.67
GeneralService1	1	N	21.4	1.51	0.959	0.991	0.009		0	21.4
(FL)	2	LN	-0.572	1.44	0.041	0.218	0.782		23.99	25.58
GeneralService2	1	N	17.08	0.94	0.728	0.973	0.027		0	17.08
(FL)	2	N	19.18	0.16	0.272	0.072	0.928		0	19.18
HCFlare (FL)	1	N	2.41	0.62	1	0			0	2.41
LowPressure	1	N	24.64	0.918	0.699	0.988	0.012		0	24.64
(FL)	2	LN	0.158	0.712	0.301	0.027	0.973		25.78	27.20
Merox	1	N	31.9	16.23	0.058	0.908	0.091		0	31.9
(FL)	2	N	500.4	89.45	0.942	0.006	0.994		0	500.4
OlefinsFlare	1	N	1.67	0.41	0.669	0.973	0.027		0	1.67
(FL)	2	LN	0.98	0.51	0.331	0.053	0.947		2.34	5.37
CoolingTower1	1	N	0.07	0.029	0.656	0.746	0.191	0.063	0	0.07
(CT)	2	LN	-2.778	1.023	0.194	0.623	0.295	0.082	0.13	0.24
	3	LN	-1.811	0.945	0.15	0.298	0.085	0.617		
CoolingTower2	1	N	0.23	0.077	0.29	0.835	0.155	0.1	0	0.23
(CT)	2	N	0.67	0.131	0.438	0.095	0.73	0.176	0	0.67
	3	LN	-1.013	0.963	0.272	0.022	0.272	0.707		
Stacks/Fugitives	1	LN	-0.15	0.56	1	NA			0	1.0068

A second approach for reducing flare emissions is to add more compressor capacity to capture more nearly constant emissions. This approach was modeled by assuming that the nearly constant component of mass flows to all flares in the HG area was reduced by 50% in magnitude. The characteristics of the stochastic inventory generator, modified for this task, are shown in Table 3. The expected values of the models for nearly constant emissions were reduced by 50%,

keeping the shape of the model distributions intact. The expected value for a normal distribution is its mean. Therefore, for modes with normal distributions, which include all of the nearly constant emission modes, except Flare 5 in Table 1, means were reduced by 50%. For example, the mean for the nearly constant emission model for Flare 1 in Table 1 were reduced from 2.43 to 1.22 as shown in Table 3. For lognormal distributions, however, expected values are a function of both mean and standard deviation (Expected value $= e^{\mu + \frac{\sigma^2}{2}}$), and the shapes of lognormal distributions are determined by both mean and standard deviation (Variance $= \left(e^{\sigma^2} - 1 \right) e^{2\mu + \sigma^2}$). Therefore, the only way to reduce expected value of lognormal distributions without changing the shape of the distribution is to move the distributions to the left by reducing shift value of the model. For nearly constant component of Flare 5 in Table 3, shift value was reduced so that expected value will be 50% of the original expected value shown in Table 1 (Expected value $= e^{\mu + \frac{\sigma^2}{2}} + shift$); when the distribution was moved to the left by -449 lbs h^{-1}, the expected value for the distribution was reduced 50%, to 491.6 lbs h^{-1}

$$(E(X)_{WO/ Control} = e^{6.8 + \frac{0.305^2}{2}} + 42.64 = 983.2, \ E(X)_{NC\ Control} = e^{6.8 + \frac{0.305^2}{2}} - 449 = 491.6).$$

Table 3. Parameters used to develop stochastic emissions with nearly constant emissions from flares reduced.

Source Name (Type)	Component	Normal or Lognormal	Mean or Mean (LN Value)	Standard deviation	Normalized proportion	Transition Matrix			Shift	Expected value
Flare1	1	N	1.22	0.26	0.603	0.883	0.115	0.001	0	1.22
(FL)	2	LN	-0.798	1.05	0.389	0.179	0.813	0.008	2.76	3.54
	3	LN	1.26	0.5	0.008	0.085	0.38	0.535	5.14	9.13
Flare2	1	N	0.99	0.64	0.544	0.798	0.196	0.005	0	0.99
(FL)	2	LN	0.54	0.97	0.426	0.252	0.729	0.02	2.81	5.56
	3	LN	-0.75	1.65	0.029	0.048	0.333	0.619	11	12.84
Flare5	1	LN	6.8	0.305	0.7632	0.951	0.022	0.027	-449	491.61
(FL)	2	N	2017	114.8	0.061	0.29	0.557	0.154	0	2017
	3	LN	5.98	0.72	0.1758	0.113	0.058	0.829	2153.2	2665.6
FCCU	1	N	10.6	3.01	0.9063	0.997	0.002	0.001	0	10.6
(FL)	2	N	33.67	2.14	0.0719	0.032	0.958	0.01	0	33.67
	3	LN	0.95	0.69	0.0217	0.003	0.058	0.939	37.56	40.84
General	1	N	10.7	1.51	0.9462	0.99	0.009	0.001	0	10.7
Service1	2	LN	-0.572	1.44	0.0402	0.218	0.762	0.02	23.99	25.58
(FL)	3	LN	0.404	1.41	0.0135	0.046	0.068	0.886	28.85	32.90
General	1	N	8.54	0.94	0.67	0.97	0.027	0.003	0	8.54
Service2	2	N	19.18	0.16	0.25	0.072	0.869	0.059	0	19.18
(FL)	3	LN	-1.61	1.48	0.08	0.022	0.186	0.792	19.48	20.08
HCF	1	N	1.21	0.62	0.974	0.989	0.011		0	1.21
(FL)	2	LN	-0.3	0.64	0.026	0.426	0.574		4.01	4.92
Low	1	N	12.32	0.918	0.6918	0.988	0.012	0	0	12.32
Pressure	2	LN	0.158	0.712	0.298	0.027	0.972	0.001	25.78	27.29
(FL)	3	LN	0.079	0.558	0.0102	0.011	0.039	0.95	34.76	36.02
Merox	1	N	16.0	16.23	0.056	0.896	0.091	0.012	0	16. 0
(FL)	2	N	500.4	89.45	0.914	0.006	0.991	0.003	0	500.4
	3	LN	4.891	0.242	0.03	0.019	0.082	0.899	622.5	759.5
Olefins	1	N	0.84	0.41	0.661	0.973	0.027	0	0	0.84
Flare	2	LN	0.98	0.51	0.327	0.053	0.944	0.003	2.34	5.37
(FL)	3	LN	0.38	1.02	0.012	0.045	0.045	0.909	16.88	19.34
Cooling	1	N	0.07	0.029	0.656	0.746	0.19	0.063	0	0.07
Tower1	2	LN	-2.778	1.023	0.194	0.623	0.295	0.082	0.13	0.24
(CT)	3	LN	-1.811	0.945	0.15	0.298	0.085	0.617	0.39	0.65
Cooling	1	N	0.23	0.077	0.29	0.835	0.155	0.01	0	0.23
Tower2	2	N	0.67	0.131	0.438	0.095	0.73	0.176	0	0.67
(CT)	3	LN	-1.013	0.963	0.272	0.022	0.272	0.707	0.86	1.44
STs/FUs	1	LN	-0.15	0.56	1	NA				1.01

Air quality modeling

The effectiveness of the control strategies, described in the previous sub-section, was assessed using the Comprehensive Air Quality Model with extensions (CAMx) (Environ, 2004). In this work, a computationally efficient version of CAMx, referred to as a sub-domain model, was used. The overall strategy in developing the sub-domain model was to (1) identify a geographical region (sub-domain) from a full, 3-D photochemical model simulation, (2) create a computationally efficient photochemical model of the sub-domain, and (3) analyze many scenarios of variable emissions using the sub-domain model. Steps 1 and 2 in the development of the model are analogous to the methods used by Nam et al. (2006) and Webster et al. (2007) and are only summarized here. Step 3 is described in the results section.

The geographical region (sub-domain) to be modeled is the HG 1 km domain, shown as the region in red in Figure 5. CAMx simulations using the full domain, shown in Figure 5, were used to develop boundary and initial conditions for the sub-domain. Details of the meteorological modeling and the VOC and NOx emission inventory development for simulation of the full domain are available from the TCEQ (2006) and were described by Nam et al. (2006). Briefly, meteorological inputs were based on results from the NCAR/Penn State Mesoscale Meteorological Model version 5, MM5. Emission inventories were prepared by the Texas Commission on Environmental Quality (TCEQ). A MOBILE6-based inventory was developed for on-road mobile source emissions. Emissions for non-road mobile and area sources were developed using the U.S. EPA's NONROAD model, using local activity data when available. Biogenic emission inventories were estimated using the GLOBEIS emission model with locally developed land cover data. Point source emissions data were developed with TCEQ's point source database and special inventory. Approximately 150 tons/day of reactive olefin species were added to approximately 100 point sources in the domain, based on ambient measurements made by aircraft (Ryerson et al., 2003). These point source inventory additions are commonly referred to as the imputed inventory, since the added emissions were estimated based on ambient measurements rather than reported inventories. The imputed point source inventory and the other components of the emission inventory, described above, were used as the base case in this work and will be collectively referred to as the deterministic inventory. Both the sub-domain modeling and the full domain modeling in the region with industrial emissions were performed at a 1 km spatial resolution.

The full domain model was used to establish initial conditions and time varying boundary conditions for the sub-domain model. Calculations reported by Nam et al. (2006) indicate that the sub-domain model responds to temporal variability in industrial emissions in a manner that correlates (r^2>0.96) with the response of the full domain model.

The sub-domain model was run for 25 August, 2000. This date was selected because there was rapid ozone formation on this date and it shows one of the typical meteorological conditions that lead to high ozone concentrations. Details of the meteorological conditions on this date have been described by Nam et al. (2006).
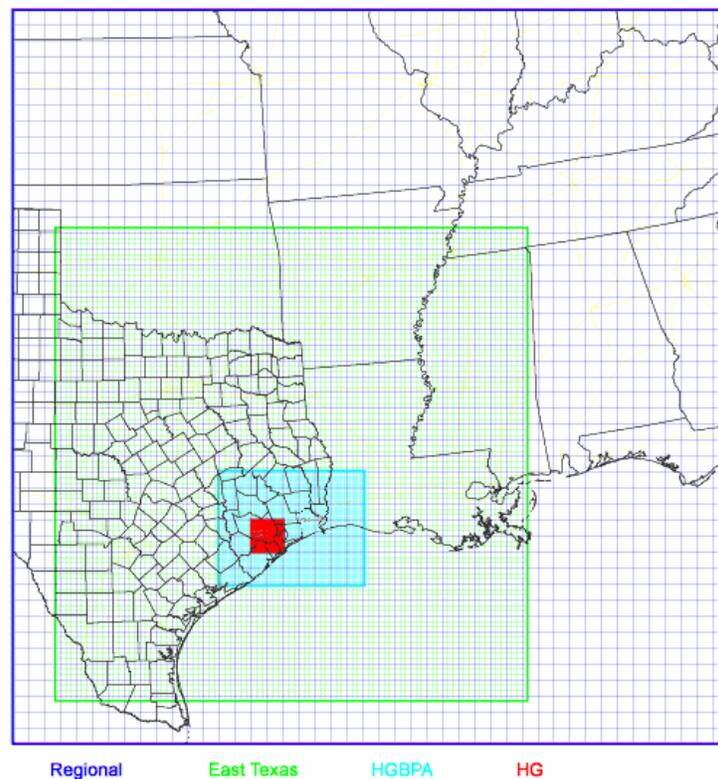
Figure 5. Modeling domain used in the study. The Regional, East Texas, Houston-Galveston-Beaumont-Port Arthur (HGBPA), and Houston Galveston (HG) nested domains had 36, 12, 4 and 1 km resolution, respectively.

Results and Discussion

The Results and Discussion will be presented in two parts. The first part describes the effectiveness of control of allowable episodic component of flare emissions and the second part describes the effectiveness of control of the nearly constant component of flare emissions.

Control of allowable episodic emissions

A total of 100 sets of stochastic emission inventories were generated with the models shown in Tables 1 and 2: 50 sets of inventories for simulation of emission variability without any emission control and 50 sets of inventories for simulation of emission variability with elimination of the allowable episodic emissions. Figure 6 compares one of the stochastic emission inventories, with no controls, to a simulation in which industrial non-EGU emissions were constant (the deterministic inventory). Figure 6 shows the differences in ozone concentrations between predictions using the 19th stochastic inventory and using the deterministic inventory. The 19th stochastic inventory led to the largest increase in ozone concentration of the 50 emission scenarios with no controls applied. Since the stochastic inventory has both higher and lower VOC emissions across the HG area over the course of the day, ozone concentrations predicted using the stochastic inventory are both higher and lower than using the deterministic inventory without VOC emission variability, depending on time of day and location. At conditions that lead to maximum difference in ozone concentration, ozone concentrations predicted using the stochastic inventory are approximately 57 ppb higher than using the deterministic inventory without variable emissions. Ozone concentrations are also up to 7 ppb lower using the stochastic inventory than using the deterministic inventory with constant industrial emissions.
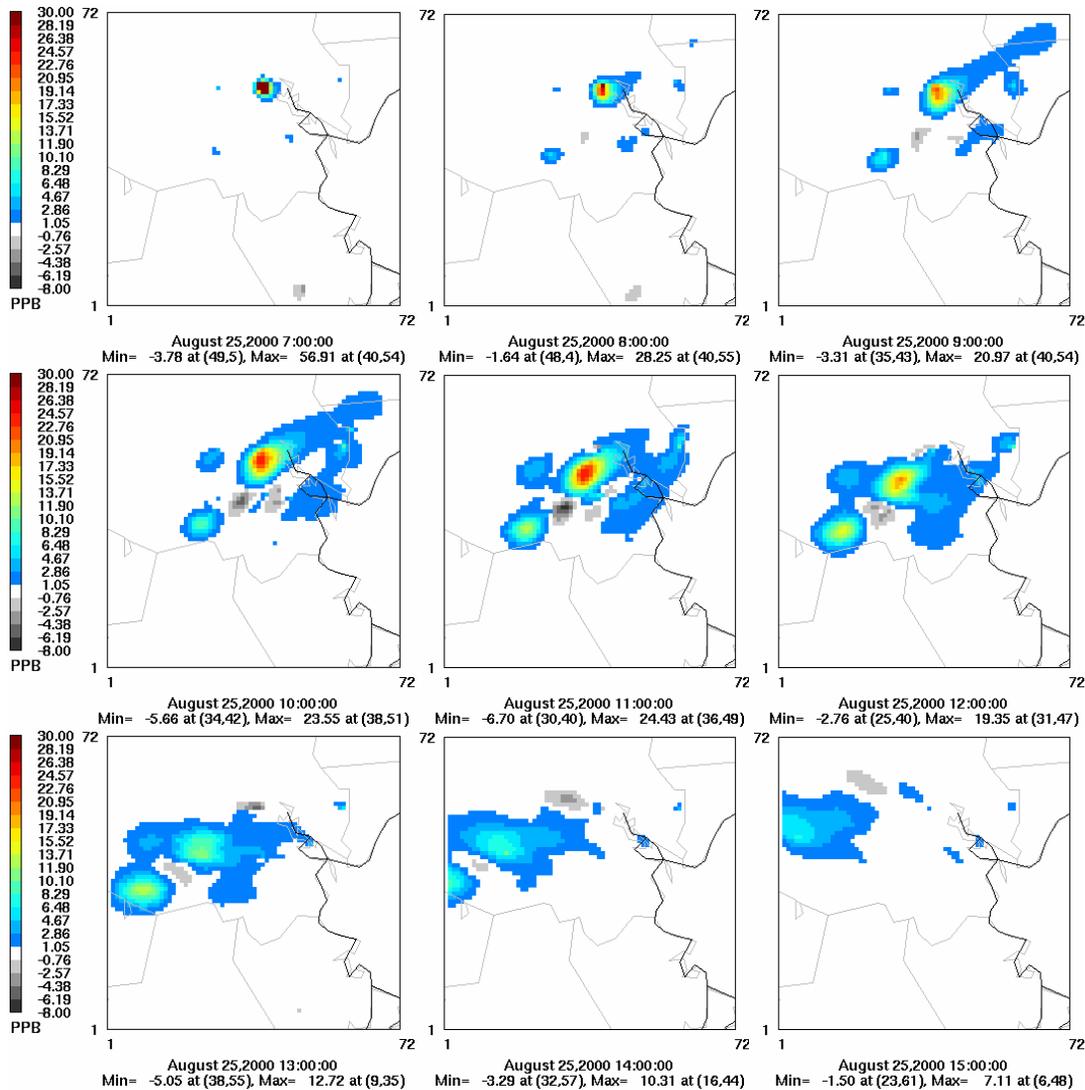
Figure 6. Difference in ozone concentrations for 25 August from 700hr to 1500hr between predictions based on the 19th stochastic inventory generated using the models shown in Table 1 and predictions based on the deterministic inventory.

Averages of the maximum difference in ozone concentrations (between the stochastic inventory with no controls and the deterministic inventories) are 24.8 ppb, over 50 simulations. Figure 7a summarizes the maximum changes in ozone concentrations, both positive and negative, when all 100 sets of stochastic emission inventories were used for air quality simulations. Specifically, the quantity presented is the maximum difference in ozone concentration over the course of the day between using the stochastic inventory and the deterministic inventory. In the simulation of ozone without any emission control, the maximum difference in ozone concentration is largest when the 19th stochastic inventory was used; the ozone concentrations

are 24.5 ppb and 81.4 ppb when the deterministic and the stochastic inventory were used, respectively, at conditions that lead to the maximum increase in ozone concentration. This result is analogous to the results shown by Webster et al. (2007), except that for this study the updated version of stochastic inventory generator was used, as described in the Methods section. Averages of the maximum difference between the stochastic and deterministic inventories reported by Webster et al. (2007) is 24.5 ppb, which is very close to the value of 24.8 ppb for modified stochastic inventory generator.

Figures 7b and 8 show results similar to that shown in Figures 6 and 7a, however, in this case, the allowable episodic flare emissions were eliminated. Figure 8 shows the difference in predicted ozone concentrations on 25 August between using the 10th stochastic inventory, generated with the models that reflect elimination of allowable episodic emissions, and using the deterministic inventory. The 10th stochastic inventory is the inventory that led to the largest increase in ozone concentration, as shown in Figure 7b. Compared to the results shown in Figure 6, ozone concentration was increased in smaller areas and decreased in larger areas due to emission variability. In addition, the magnitude of increase in ozone concentration was smaller and the magnitude of decrease was larger. Averages of the maximum difference in ozone concentrations (between the stochastic inventory with allowable episodic emission controls and the deterministic inventories) are 18.2 ppb, over 50 simulations. The probability distributions of maximum difference in ozone concentration, both positive and negative, are shown in Figure 9. The distribution of maximum increases in ozone concentration, shown in Figure 9a, has shorter tail to the right for the case when allowable episodic emissions are eliminated, as compared to the stochastic inventory results with no controls.
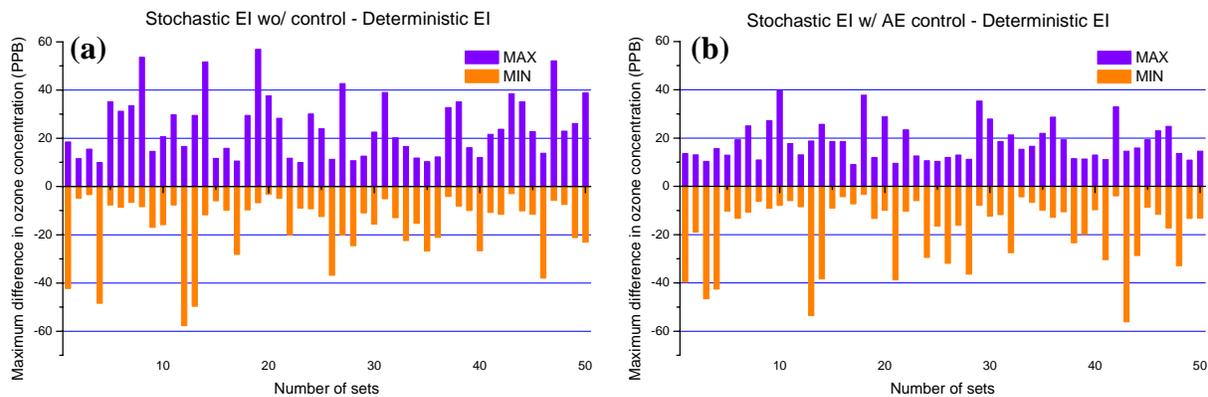
Figure 7. Maximum difference in ozone concentration in one day simulations representing 25 August, 2000. The difference is taken between the deterministic inventory with constant industrial emissions and the stochastic inventory for 50 instances of the stochastic inventory with allowable episodic emission without control (a) and with control (b).
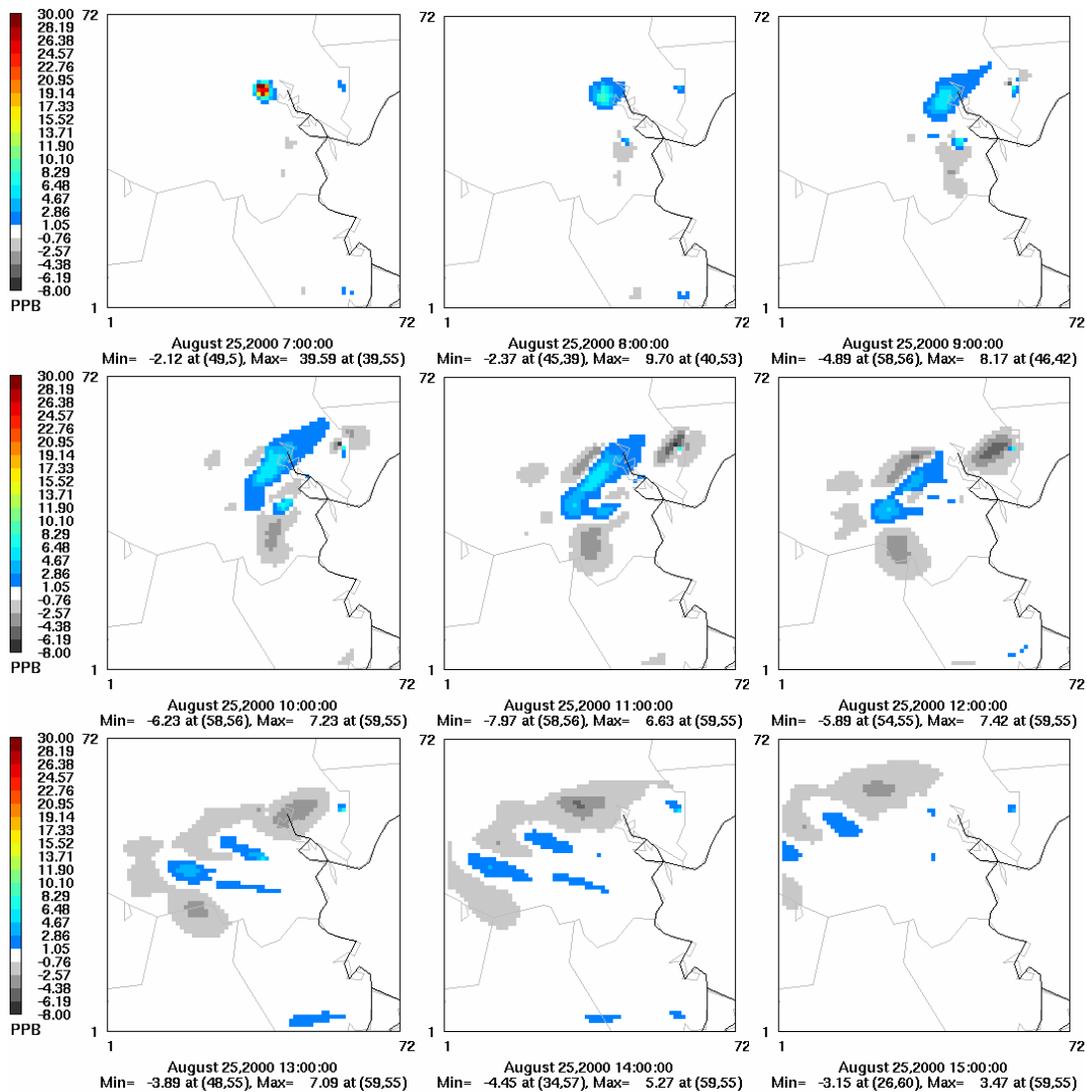
Figure 8. Difference in ozone concentration for 25 August from 700hr to 1500hr between predictions based on the 10th stochastic inventory generated using the models shown in Table 2 and predictions based on the deterministic inventory. Ozone concentrations are scaled to the results shown in Figure 6.
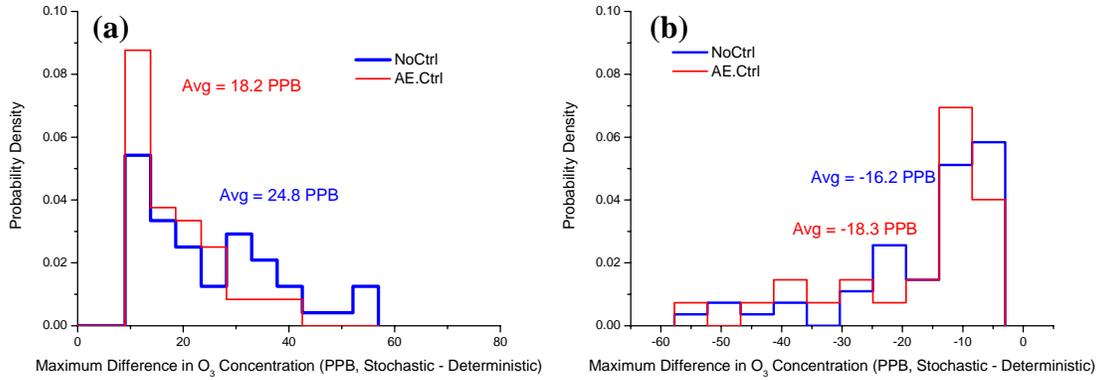
Figure 9. Probability distribution of maximum changes in ozone concentration in simulations representing 25 August, 2000 due to variable continuous emissions with allowable episodic emission control (red line) and without the control (blue line) in positive direction (a) and negative direction (b).

Figure 10 compares area-wide, daily maximum ozone concentrations, across the HG 1-km domain, using the stochastic inventories with no controls and the stochastic inventories with allowable episodic emissions control. For stochastic inventories without any emission control, the daily maximum ozone concentration ranges from 193.9 ppb to 206.5 ppb, depending on the stochastic inventory used. The average of daily maximum ozone concentration using the 50 sets of stochastic inventories is 200.9 ppb (the area-wide maximum for the deterministic inventory was 200.6 ppb). For stochastic inventories with allowable episodic emissions eliminated, the daily maximum ozone concentration ranges from 193.3 ppb to 204 ppb, depending on the stochastic inventory used. The average of the daily maximum ozone concentration with controls was 199.4 ppb, approximately 1.5 ppb decrease from the average of daily maxima without any emission control.
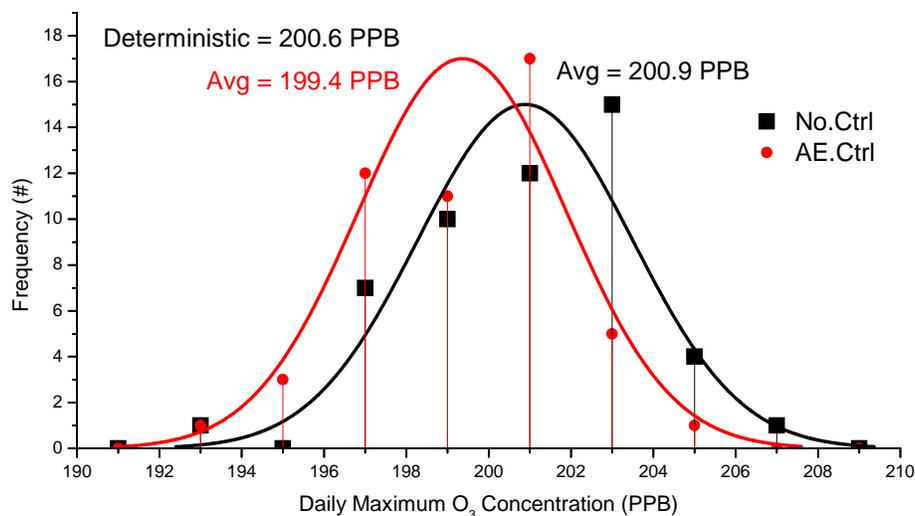
Figure 10. Distributions of daily maximum ozone concentration across the HG 1-km domain for no control cases (black) and allowable episodic emission control cases (red).

For comparison purposes, another control scheme was devised so that the same magnitude of reduction in total flare emissions occurred across the domain as when allowable episodic emissions are eliminated, but those reductions are applied to the deterministic inventory. This results in 2.1% and 4.3%, reductions in NOx and VOC emissions, respectively. Figure 11 shows differences in ozone concentrations between using the reduced deterministic inventory and using the deterministic inventory. Changes in ozone concentration due to the overall reduction are not significant compared to the results shown in Figures 7b and 8. The maximum difference in ozone concentration was approximately 1.4 ppb. Daily maximum ozone concentration was decreased by just 0.1 ppb due to the emissions reductions in the deterministic inventory. This reduction in daily maximum ozone is smaller, by a factor of 11, than the average reduction in daily maximum ozone concentration (200.9 vs. 199.4 ppb, or 1.5 ppb) due to an equivalent mass reduction in allowable episodic emissions, as shown in Figure 10.
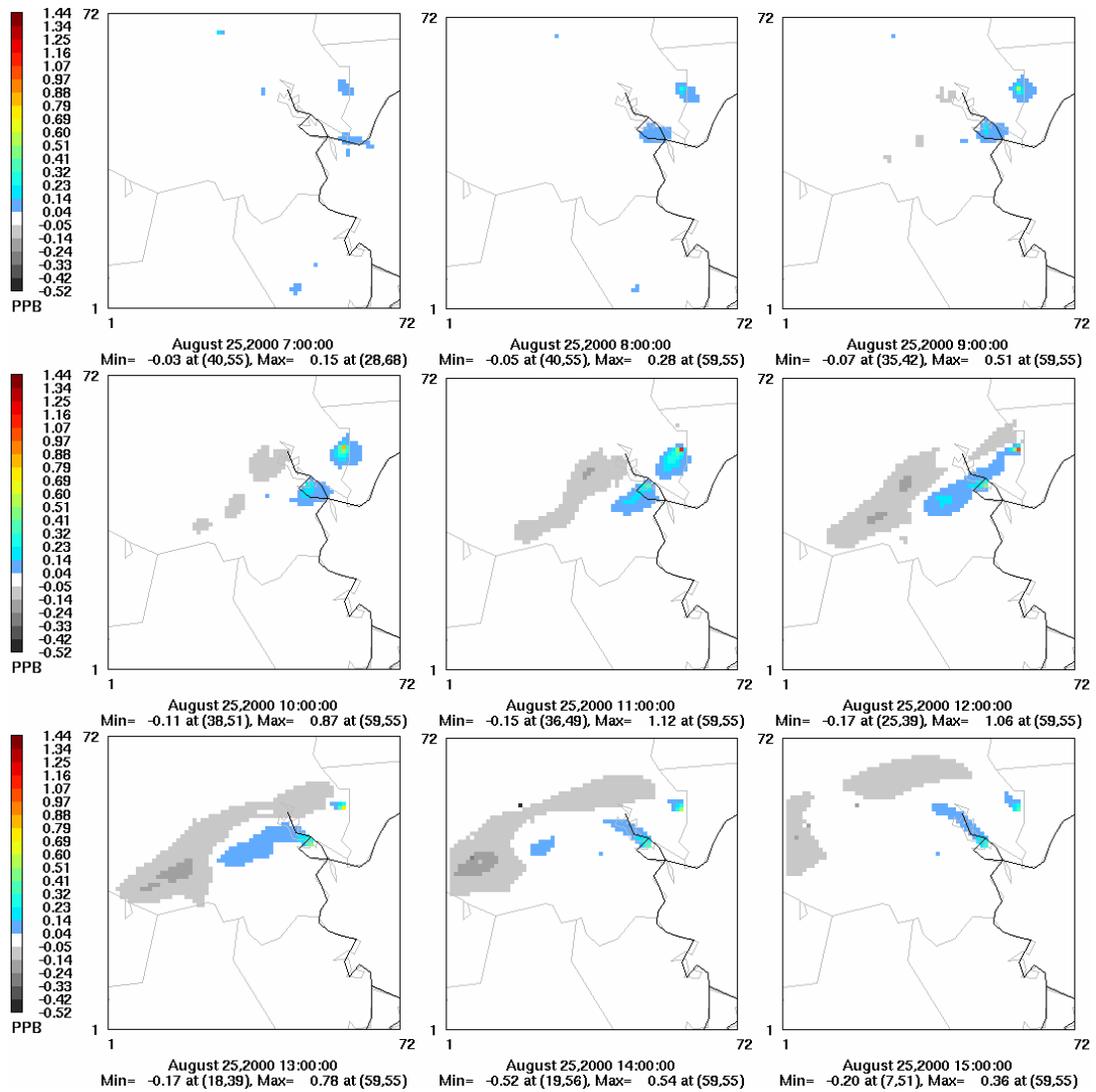
Figure 11. Difference in ozone concentration for 25 August from 700hr to 1500hr between predictions based on the reduced deterministic inventory and predictions based on the deterministic inventory. Percentage reduction in emissions was same with that from allowable episodic emission control. Maximum difference, approximately 1.4 ppb, occurred at 2000hr.

Control of nearly constant emissions

The second control approach involves reduction in nearly constant emissions of NOx and VOC emissions for all the flares in the HG domain. The stochastic inventory generator was modified to reflect this control scheme, as shown in Table 3, and a total of 50 sets of stochastic emission inventories were generated with the models. As described in the previous section, expected values of the nearly constant emissions were decreased by 50% by reducing means or shift values, depending on the distribution type (normal or lognormal). Figure 12 shows the difference in ozone concentration between using the 38th stochastic inventory with 50% reduction in nearly constant emissions and using the deterministic imputed inventory. The 38th stochastic inventory is the inventory that led to largest additional ozone formation as shown in Figure 13. Compared to the results shown in Figure 6 (base case stochastic inventory), ozone concentration was increased in smaller areas and decreased in larger areas over the course of the day.

Figure 13 summarizes the maximum changes in ozone concentrations, both positive and negative, when the 50 sets of stochastic emission inventories with a 50% reduction in nearly constant flare emissions were used for simulations. The maximum difference in ozone concentration is largest when the 38th stochastic inventory was used; the ozone concentrations are 47.4 ppb and 98.1 ppb when the deterministic and the stochastic inventory were used, respectively, at conditions that lead to the maximum increase in ozone concentration. Figure 14 compares the maximum difference in ozone concentration, both positive and negative, for eliminating allowable episodic emissions, for 50% reduction in nearly constant emissions, and for no control cases. Controlling the nearly constant emissions is not as effective in eliminating large maximum increases in ozone as controlling the allowable episodic emissions, however, reducing nearly constant emissions generates larger maximum decreases in ozone concentrations.
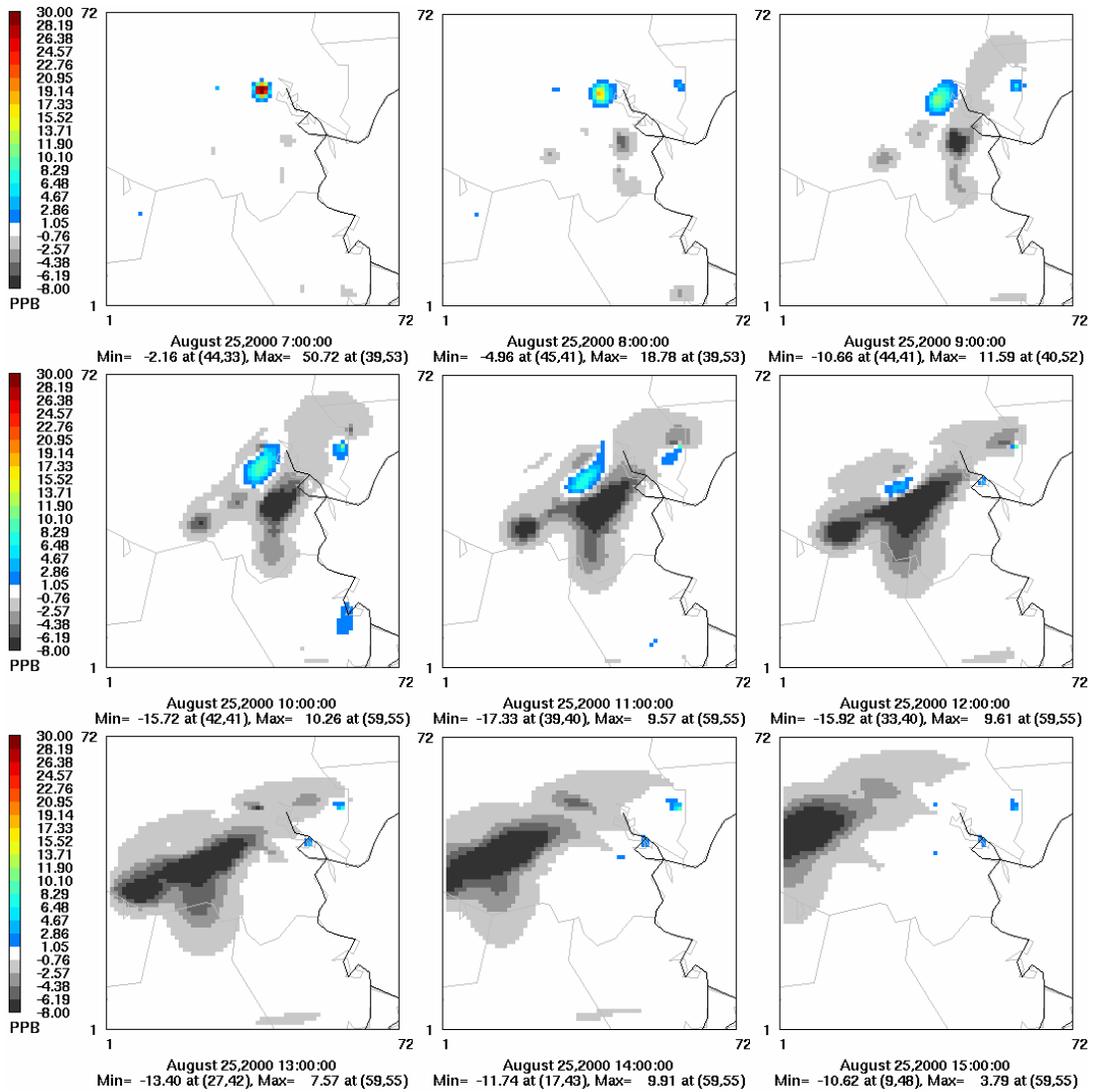
24

Figure 12. Difference in ozone concentration for 25 August from 700hr to 1500hr between predictions based on the 38th stochastic inventory generated using the models shown in Table 3 and predictions based on the deterministic inventory. Ozone concentrations are scaled to the results shown in Figures 6 and 7.
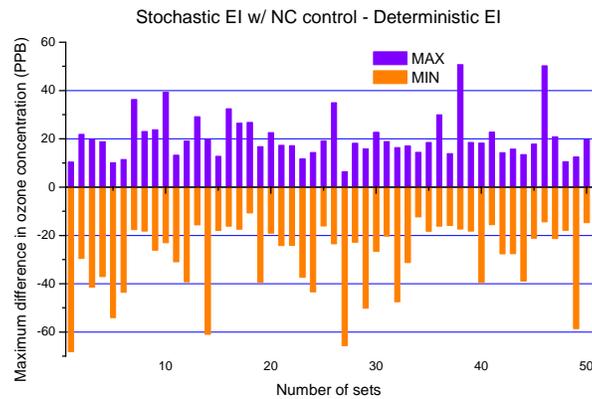
Figure 13. Maximum difference in ozone concentration in one day simulations representing 25 August, 2000. The difference is taken between the deterministic inventory with constant industrial emissions and the stochastic inventory for 50 instances of the stochastic inventory with a 50% reduction in nearly constant flare emissions. Maximum difference in ozone concentration was scaled to the results shown in Figure 7.
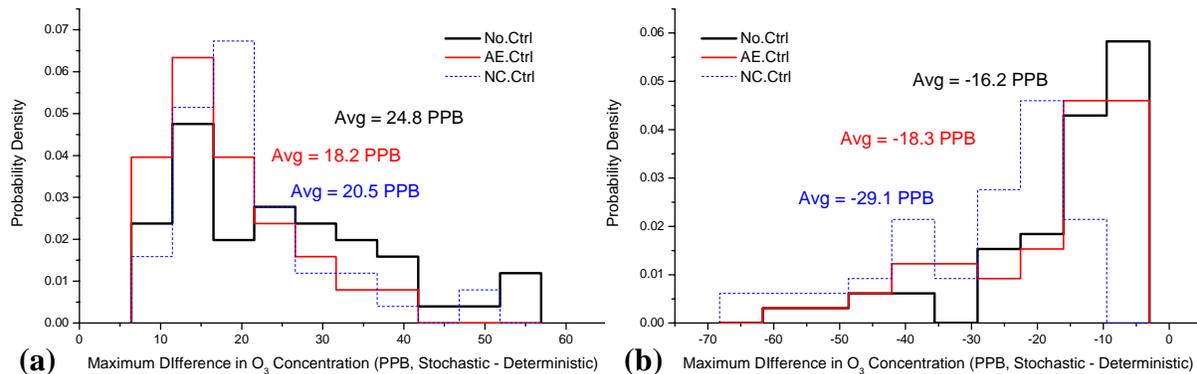

Figure 14. Probability distributions of maximum changes in ozone concentration in simulations representing 25 August, 2000 due to variable continuous emissions with allowable episodic emission control (red line), with nearly constant emission control (blue line) and without the control (black line) in positive direction (a) and negative direction (b).

Figure 15 compares daily maximum ozone concentration in the HG domain for no control, for allowable episodic emission control, and for nearly constant emission control cases. Control of nearly constant emissions reduces the average peak ozone concentration by 10.5 ppb, versus a 1.5 ppb reduction for the control of allowable episodic emissions, however, the tons of

emission reductions are different in the two cases. On average, total flare emissions across the domain were decreased, due to control of allowable episodic emissions, by 1.4 tons and 0.12 tons for VOC and NOx, respectively, relative to no control cases. Reduction in daily maximum ozone concentration due to the control is 1. ppb per ton of VOC plus NOx reduction (1.5 ppb / 1.5 tons). Control of nearly constant emissions reduced total flare emissions by 9.73 tons and 1.47 tons, for VOC and NOx, respectively. Reduction in daily maximum ozone concentration is 0.9 ppb per ton of VOC plus NOx reduction (10.5 ppb / 11.2 tons). Thus, the two strategies are equally effective, per ton, in reducing average peak ozone concentration. More mass of nearly constant emissions is available for reductions, however, so these emissions provide a larger potential for change in average daily maximum ozone concentrations. As shown in Figure 14, however, for eliminating the highest values of localized changes in ozone concentrations, reducing allowable episodic emissions is a more effective strategy than reducing nearly constant emissions.
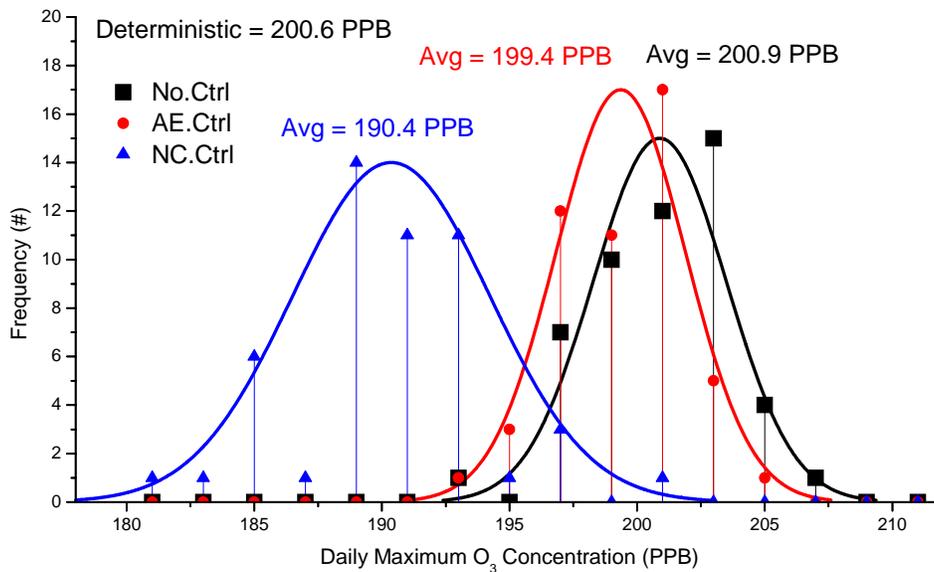

Figure 15. Histograms of daily maximum ozone concentration across the HG 1-km domain for no control cases (black), allowable episodic emission control cases (red), and nearly constant emission control cases (blue).

For comparison purposes, the same magnitude of reduction in total flare emissions, due to nearly constant emission control, were applied to the deterministic inventory. Figure 16 shows difference in ozone concentration between using the reduced deterministic inventory and using the deterministic inventory. Daily maximum ozone concentration using the reduced deterministic inventory was about 198.7 ppb, approximately 1.9 ppb lower than using the base case deterministic inventory. This decrease in daily maximum ozone concentration was more than a factor of 5 smaller than the average decrease in daily maximum ozone shown in Figure 15.
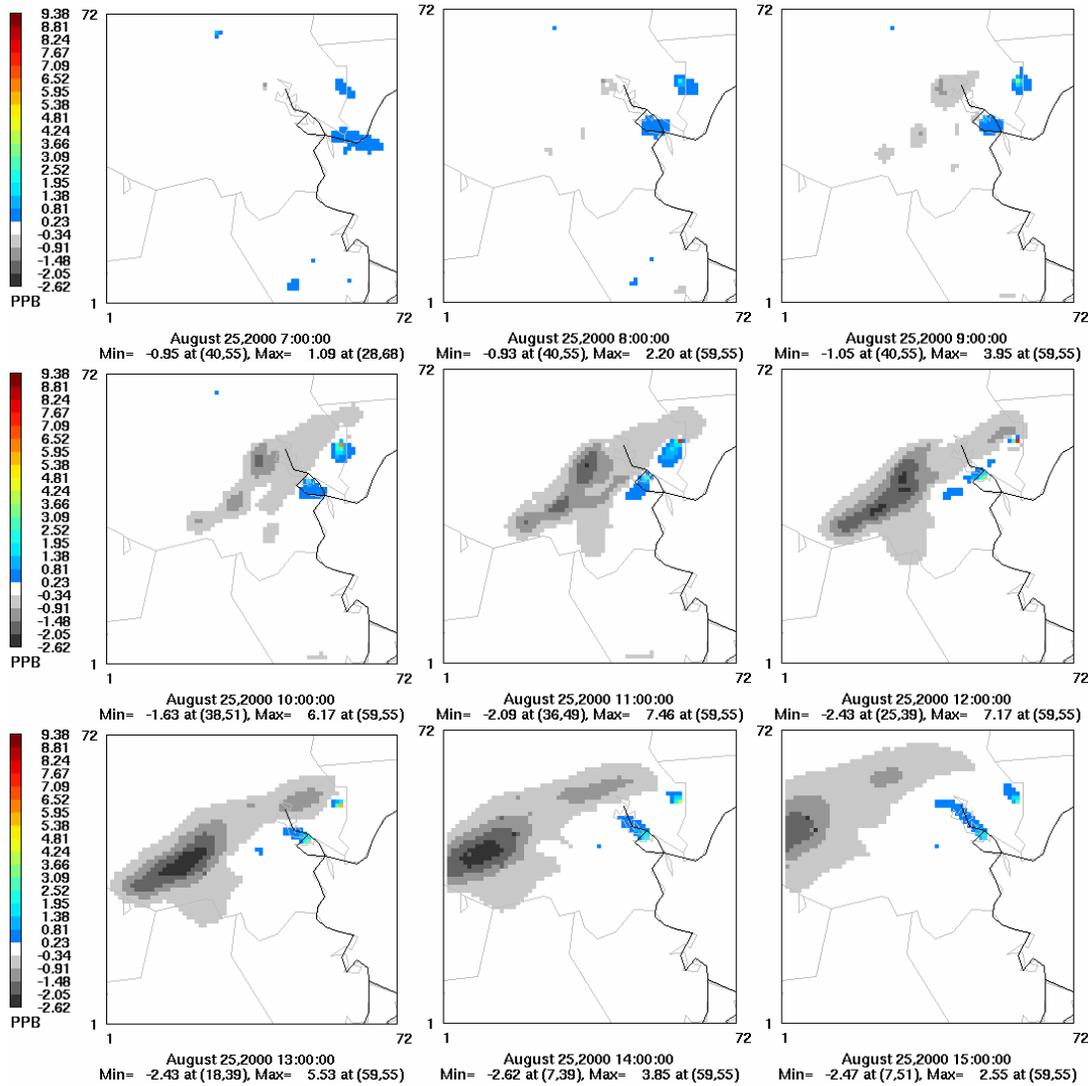

Figure 16. Difference in ozone concentration for 25 August from 700hr to 1500hr between predictions based on the reduced deterministic inventory and predictions based on the deterministic inventory. Percentage reduction in emissions was same with that from nearly

constant emission control. Maximum difference, approximately 9.4 ppb, occurred in (59, 55) at 2000hr.

(a) Maximum DIfference in O_3 Concentration (PPB, Stochastic - Deterministic)

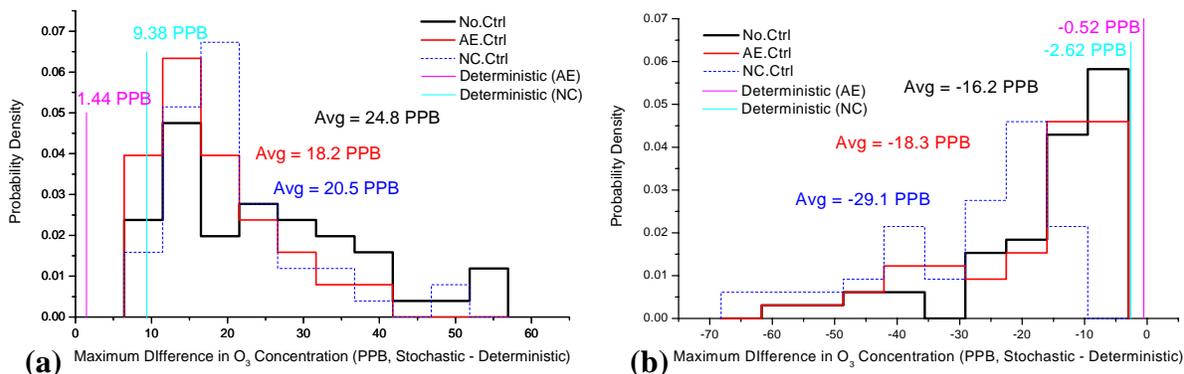**(b)** Maximum DIfference in O_3 Concentration (PPB, Stochastic - Deterministic)

Figure 17. Probability distributions of maximum changes in ozone concentration in simulations representing 25 August, 2000 due to various emission controls in the stochastic inventory and due to the equivalent reductions applied to deterministic inventory in positive direction (a) and negative direction (b).

Conclusions

This study evaluated two flare reduction scenarios as examples of alternative strategies for reducing ozone concentrations due to variable industrial emissions. The first control strategy involved reducing large magnitude, infrequent emissions (allowable episodic emissions) from flares and the second strategy involved reducing continuous, and relatively constant, emissions (nearly constant emissions) from flares.

In reducing changes in the daily maximum ozone concentrations, over the 1-km domain shown in Figure 5, the two strategies are equally effective, per ton, in reducing average peak ozone concentration. More mass of nearly constant emissions is available for reductions, however, so these emissions provide a larger potential for change in average daily maximum ozone concentrations. In contrast, for eliminating the highest values of localized changes in ozone concentrations, reducing allowable episodic emissions is a more effective strategy than reducing nearly constant emissions. For both control cases, maximum increases and decreases in ozone concentrations were significantly larger than those due to equivalent reductions in VOC and NOx emissions applied to deterministic inventories.

References

Bay Area Air Quality Management District (BAAQMD), 2005. Flare Monitoring at Petroleum Refineries, Accessed January 2007 at http://www.baaqmd.gov/dst/regulations/rg1211.pdf

Bay Area Air Quality Management District (BAAQMD), 2006. Flares at Petroleum Refineries, Accessed January 2007 at http://www.baaqmd.gov/dst/regulations/rg1212.pdf

Kleinman, L.I., Daum, P.H., Imre, D., Lee, Y.N., Nunnermacker, L.J., Springston, S.R., Weinstein-Lloyd, J., Rudolph, J., 2003. Correction to "Ozone production rate and hydrocarbon reactivity in 5 urban areas: A cause of high ozone concentration in Houston". Geophys. Res. Lett. 30 (12), 1639.

Levy, R.E., Randel, L., Healy, M., Weaver, D. 2006. Reducing emissions from plant flares. *Proceedings of the Air & Waste Management Association's Annual conference*, Paper #61.

Murphy, C.F., Allen, D.T., 2005. Hydrocarbon emissions from industrial release events in the Houston-Galveston area and their impact on ozone formation. Atmospheric Environment 39(21), 3785-3798.

Nam, J., Kimura, Y., Vizuete, W., Murphy, C.F., Allen, D.T., 2006. Modeling the impacts of emission events on ozone formation in Houston, Texas. Atmospheric Environment 40 (28), 5329-5341.

Ryerson, T.B., Trainer, M., Angevine, W.M., Brock, C.A., Dissly, R.W., Fehsenfeld, F.C., Frost, G.J., Goldan, P.D., Holloway, J.S., Hubler, G., Jakoubek, R.O., Kuster, W.C., Neuman, J.A., Nicks, D.K., Parrish, D.D., Roberts, J.M., Sueper, D.T., Atlas, E.L., Donnelly, S.G., Flocke, F., Fried, A., Potter, W.T., Schauffler, S., Stroud, V., Weinheimer, A.J., Wert, B.P., Wiedinmyer, C., Alvarez, R.J., Banta, R.M., Darby, L.S., Senff, C.J., 2003. Effect of petrochemical industrial emissions of reactive alkenes and NOx on tropospheric ozone formation in Houston, Texas. J. Geophys. Res. 108 (D8), 4249.

Shell Oil Products US, 2006. Shell Martinez Refinery Flare Minimization Plan, submitted to Bay Area Air Quality Management District, September 2006

Texas Commissions on Environmental Quality (TCEQ), 2004. Revisions to the State Implementation Plan for the Houston-Galveston-Brazoria nonattainment area. Accessed February 2007 at http://www.tceq.state.tx.us/assets/public/implementation/air/sip/sipdocs/2004-05-HGB/execsumm.pdf

Vizuete, W., 2005. Implementation of Process Analysis in a three dimensional air quality model, PhD thesis, University of Texas.

Webster, M., 2007. Personal communication

Webster, M., Nam, J., Kimura, Y., Jeffries, H., Vizuete, W., Allen, D.T., 2007. The effect of variability in industrial emissions on ozone formation in Houston, Texas. Submitted to <u>Atmospheric Environment</u>